IEEE Access
Multidisciplinary | Rapid Review | Open Access Journal

Received September 6, 2017, accepted October 19, 2017, date of publication October 25, 2017, date of current version April 18, 2018.

Digital Object Identifier 10.1109/ACCESS.2017.2766293

Multi-Mode Bandpass Cavity Filters and Duplexer With Slot Mixed-Coupling Structure

BING-LONG ZHENG[1], SAI-WAI WONG[2], (Senior Member, IEEE), SHI-FEN FENG[1], (Student Member, IEEE), LEI ZHU[3], (Fellow, IEEE), AND YANG YANG[4], (Member, IEEE)

[1]School of Electronic and Information Engineering, South China University of Technology, Guangzhou City 510640, China
[2]College of Information Engineering, Shenzhen University, Shenzhen 518060, China
[3]Department of Electrical and Computer Engineering, Faculty of Science and Technology, University of Macau, Zhuhai 999078, China
[4]School of Electrical and Data Engineering, University of Technology Sydney, Ultimo, NSW 2007, Australia

Corresponding author: Sai-Wai Wong (wongsaiwai@ieee.org)

This work was supported in part by the Shenzhen University Research Startup Project of New Staff under Grant 2018082, in part by the Department of Education of Guangdong Province Innovative Project under Grant 2015KTSCX010, in part by the Fundamental Research Funds for the Central Universities under Grant 2017ZD044, and in part by the Guangzhou Science and Technology Project under Grant 201604016127.

ABSTRACT The quasi-elliptic multi-mode bandpass cavity filters and duplexer with slot mixed-coupling structure are proposed in this paper. A single metal cavity embedded with a rectangular- shaped slot-cut metal plate is utilized to constitute a multi-mode bandpass filter with a few features including wide passband, low profile and controllable transmission zeros (TZs). In this paper, the slot-cut metal plane serves as the multi-mode resonators. In detail, the slot on the metal plane functions as the circuit element to move the higher order modes within the reasonable frequency-band, while serving as a mixed-coupling structure to generate out-of-band transmission zeros. To demonstrate the multiple-mode capability in filter design, the dual-mode, triple-mode, and quadruple-mode filters are developed by appropriately allocating a few TZs in the upper stopbands using the proposed slot mixed-coupling approach, namely, Type-I filters. Next, a quadruple-mode cavity filter with both lower and higher TZs is designed, namely, Type-II filter, which is further applied for the exploration of a duplexer. Finally, the filter and duplexer prototypes are fabricated and measured. The measurement results are found in good agreement with the simulated ones.

INDEX TERMS Multi-mode cavity filter, duplexer, mixed coupling, controllable transmission zeros.

I. INTRODUCTION

With the rapid development of mobile and satellite communication systems, the cavity filters with excellent frequency selectivity, low insertion loss, broad bandwidth, controllable frequency-bands, and miniaturized profile are in severe demand. As a traditional approach, the multiple mode resonator (MMR) technology has been well utilized for filter designs with compact size [1], [2] and sharp roll-off by applying finite transmission zeros (TZ) in the attenuation band [3], [4].

To construct a multi-mode cavity filter, most of the works use the perturbation elements to provide the extra degeneration mode in one single cavity, such as screws [5], [6], corner cuts [7], [8] and irises [9], [10]. Recently, the cylindrical dielectric [11] and cylindrical metal blocks [12] are placed in the off-center on the bottom of a cavity to separate the degenerate modes, and further achieve triple-mode filters. The quadruple-mode filter is created using four coaxial structures in a single cavity [13]. All the aforementioned works use various physical structures to excite the required additional resonant modes. In this paper, an alternative method is introduced to construct the multi-mode cavity filter by making use of the higher harmonic modes of a cavity resonator.

As we know, the frequency-selectivity and out-of-band suppression are nowadays the two main challenges in the field of multi-mode filter designs. To the best of the authors knowledge, the controllable multi-TZs in a multi-mode cavity filter is rarely elaborated, except [13], [14]. These two reported works present the method of effective control of the TZs positions by virtue of the parallel-coupling [13] and cross-coupling [14], respectively. Particularly, the TZs in either the higher or lower stopband can be controlled by adjusting the amplitude of each parallel-coupling path or the usage of electric/magnetic property of cross-coupling path. In this

paper, the alternative method that mixed-coupling technology is utilized to generate transmission zeros. The work in [15] achieves the mixed coupling on substrate integrated waveguide (SIW) through inductive window and embedded short-ended conducting strip. In [16], an inline coaxial cavity filter is constituted by using the conducting strip and metallic caps to control the electric and magnetic coupling. The above mentioned methods are quite complicated for mixed-coupling generation and not suitable for low profile metal waveguide cavity filter.

In this paper, a mixed-coupling structure is proposed, for the first time, to generate the TZs of multi-mode filters. The slot-cut on the metallic plane is presented as the mixed-coupling structure controlling the resonant frequencies of higher order modes. To verify the proposed approach, a mixed-coupling structure based multiple mode resonator is presented with a class of filters and duplexers as design examples.

The paper is organized in the following way: in Section II, the resonant modes and transmission zeros are extensively studied to formulate a proposed multi-mode resonator. In Section III, a class of multi-mode filters with TZs in the upper-stopband, namely Type-I, is designed. Section IV demonstrates a quadruple-mode filter with out-of-band suppression by locating a few TZs in both the lower- and upper-stopbands, namely Type-II. Section V presents a duplexer based on the proposed filter, followed with conclusions of the work in Section VI.

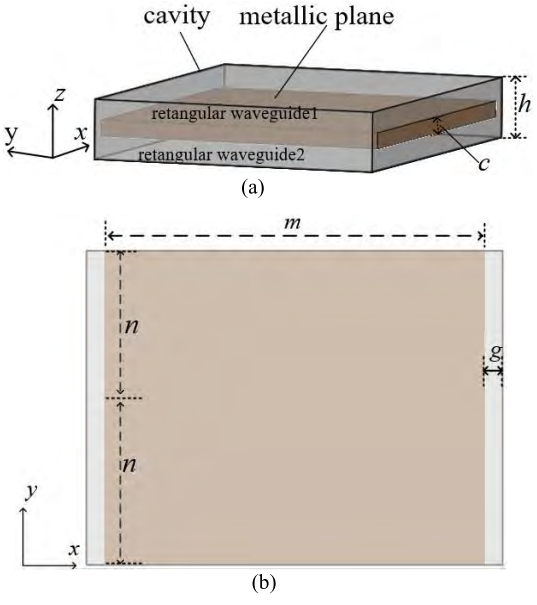

FIGURE 1. Configuration of the proposed multi-mode resonator: (a) three-dimensional view. (b) top view.

II. MULTIPLE MODE RESONATOR ANALYSIS

A. MULTI-MODE RESONATOR

Fig. 1(a) and 1(b) depicts the 3-D view and top view of a cavity embedded with a rectangular metallic plane. The metallic plane is shorted with the cavity along y-axis and is opened along x-axis with two air gaps. In its cross-section view, the metallic plane divides the cavity into two identical rectangular waveguides. In Fig. 1, the symbols, m, n, c, g and h, represent the length, width and thickness of the metal plane, the gap width, and height of the metal cavity, respectively. Herein, c, g and h are readily set as 2 mm, 2 mm, and 7.2 mm, respectively. To excite the multi-mode resonance using the proposed structure, the modes analysis are comprehensively investigated. The attribution of the electric-field for the first four eigen modes are extracted at the plane ($z = -2$ mm) as shown in Fig. 2.

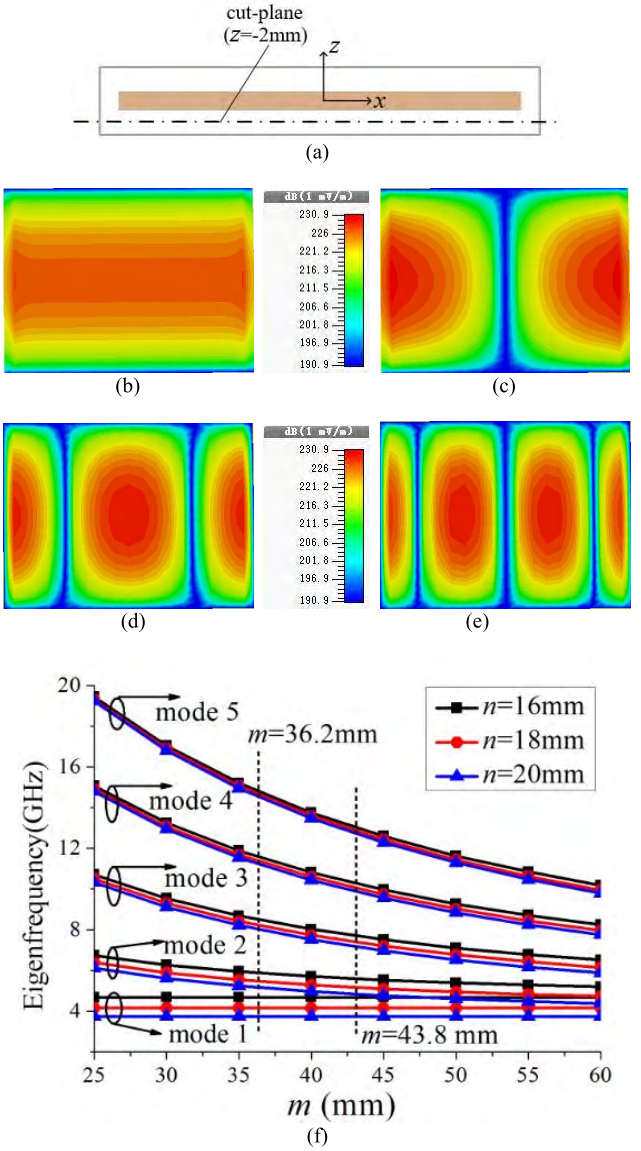

FIGURE 2. (a) Cutting plane for displaying the field distribution. (b) Electric-field distribution of TE_{100} mode for absolute value. (c) Electric-field distribution of TE_{101} mode for absolute value. (d) Electric-field distribution of TE_{102} mode for absolute value. (e) Electric-field distribution of TE_{103} mode for absolute value. (f) The resonant frequency of five modes against varied m and n.

From Fig. 2, it is apparent that the proposed structure has the fundamental mode (mode 1) and the higher

modes, namely, mode 2, mode 3 and mode 4, as shown in Fig.2 (b)-(e), respectively. The fundamental mode (mode 1) is TE_{100} mode with its electric-field distribution as indicated in Fig. 2(b). It is noteworthy that mode 1 is almost independent of the length m as shown in Fig. 2(f). The higher order mode 2, 3, and 4 are corresponding to TE_{101}, TE_{102}, and TE_{103} modes, respectively. Moreover, the TE_{101}, TE_{102} and TE_{103} modes are the conventional waveguide resonant modes existing in both waveguide 1 and waveguide 2 as depicted in Fig. 1(a). In this paper, only the first four resonant modes will be utilized to form up the desired passband. Thus, it is critical to explore the mechanism for flexible control of these resonant frequencies. It can be seen from Fig. 2(f) that the resonant frequency of TE_{100} mode can be slightly controlled by the width of the metal plane (n) but not affected by the length of the plane (m). In contrast, the higher order modes (TE_{101}, TE_{102}, TE_{103}) are certainly shifted to their respective lower frequencies as the length of plane (m) increases. In general, the uniform structure in Fig. 1 is difficult to build up a multi-mode filter because the resonant frequencies of the four modes are hardly controlled in the degree of freedom to make the higher order resonant modes close enough to the fundamental mode. Meanwhile the structure in Fig. 1 has the intrinsic disadvantage of lack-of-transmission-zeros for out-of-band harmonics suppression. To solve problem, the slot-cut is put on the middle metallic plane as a reactance loading as shown in Fig. 3(a). This slot-cut further allows us to control the resonant frequencies of these higher order modes and the mode-to-mode coupling degrees. To validate the proposed concept, the metallic planes symmetrically loaded with one, two and three slots, are investigated.

In Fig. 3, a single slot-cut is placed in the middle of the metallic plane. The resonant frequencies of mode 2 (TE_{101}) and mode 4 (TE_{103}) are shifted to the lower band as the length of the slot (a) increases. The slot width (b) has the effect on its performance but it is not remarkable. Since the mode 1 and mode 3 are independent of a, it is possible to make the mode 1 and mode 2 close to each other to form a dual-mode passband when a is approaching 18 mm.

In Fig. 4, two slot-cuts are placed on the metallic plane, and the distance between two slots is set as s. Herein, with an increasing length (a) of the two slots, the resonant frequencies of mode 2 (TE_{101}) and mode 3 (TE_{102}) shift to the lower band. Meanwhile, the frequencies of the mode 1 and mode 2 remain almost unchanged. If s is enlarged, the frequency of mode 3 is shifted to the lower band, while the mode 4 (TE_{103}) appears remarkable frequency-shift towards the higher band.

In Fig. 5, three slot-cuts (one $slot_1$ and two $slot_2$) are placed on the metallic plane, and the $slot_2$ has the shift with a distance (s) from center. In detail, the length, width of $slot_1$ and the length and width of $slot_2$ are signed as a_1, b_1, a_2 and b_2, respectively. The resonant frequencies of the first four modes change with varying parameters as shown in Fig. 5. As a_1 increases, the resonant frequencies of mode 2 and mode 3 shift to the lower band. When a_2 is enlarged, the

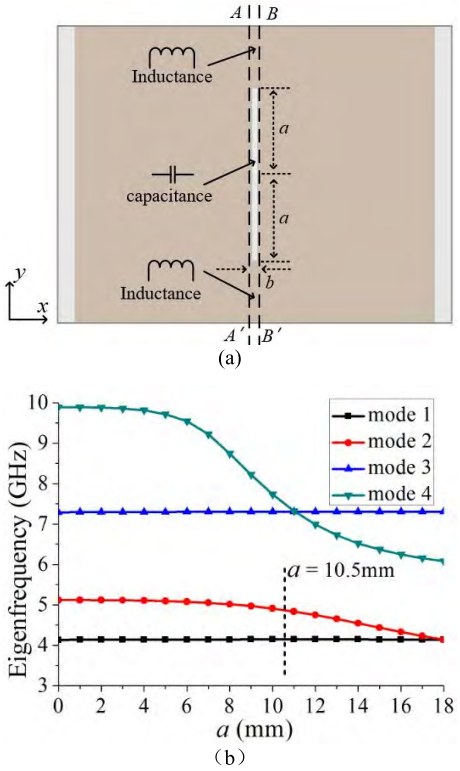

FIGURE 3. One slot loaded on the metallic plane: (a) top view of structure, and (b) resonant mode frequencies with varying *a when b* = 1.4*mm*.

resonant frequencies of mode 3 and mode 4 shift to the lower band. In terms of mode 5, the frequency is shifted away from the first four modes by adjusting s. As such, it can provide a wide upper-stopband for the fourth-order MMR filter.

According to the above discussion, the structures in Fig. 3(a), Fig. 4(a) and Fig. 5(a) can be utilized to construct the dual-, triple- and quad-mode bandpass filters with the use of proper lumped elements circuit models, respectively.

B. TRANSMISSION ZEROS

As shown in Fig. 3(a), the portion between the plane A-A' and the plane B-B' indicates the slot structure. It is apparent that the slot structure can generate the transmission zero in filter design, and herein, the slot structure is analyzed by a lumped circuit model as shown in Fig. 3(a). The parallel connection of the inductance (L) and capacitance (C) in transmission path can generate the transmission zero when the resonance condition occurs in the parallel circuit. In this structure, as the slot length increases, the values of inductance (L) and capacitance (C) are enlarged, thus the transmission zero locates on the lower frequency due to the frequency of TZ $f_Z = 1/\sqrt{LC}$.

To assure that the proposed slot structure has an out-of-band mixed coupling behavior with controllable TZs, we extract the ABCD-parameters of A-A' and B-B' section as shown in Fig. 3(a). The extracted ABCD-matrix is converted to admittance parameter Y_{21}. The imaginary-part of Y_{21} versus frequency with respect to the varying slot length

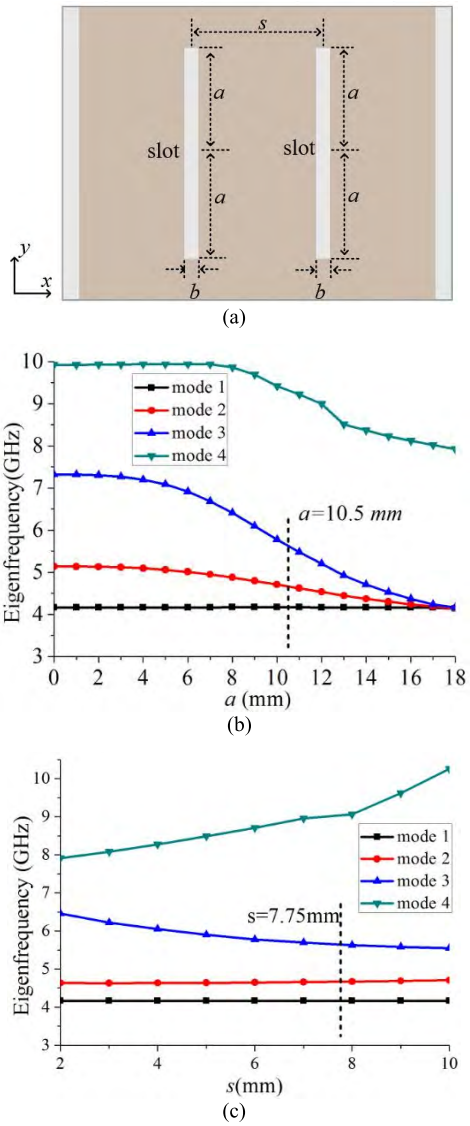

FIGURE 4. Two slots loaded on the metallic plane: (a) top view of the structure, (b) resonant mode frequencies with varying a when $b = 1.8mm$ and $s = 7.75mm$, and (c) resonant mode frequencies with varying s when $a = 10.5mm$ and $b = 1.8mm$.

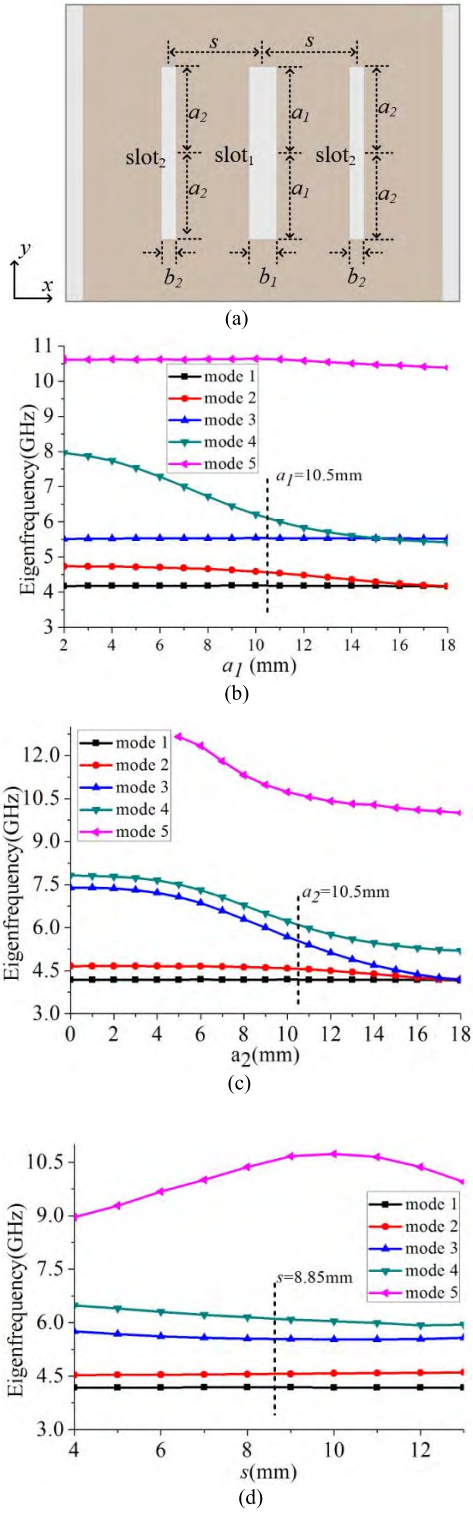

FIGURE 5. Three slots loaded on the metallic plane when $b_1 = 3.4\ mm$, $b_2 = 1.8\ mm$: (a) top view of the proposed structure. (b) resonant frequencies with varying a_1 when $a_2 = 10.5mm$. (c) resonant frequencies with varying a_2 when $a_1 = 10.5mm$, and (d) resonant frequencies with varying b_1.

is displayed in Fig. 6. It is apparent that the curves in the region of $\text{img}(Y_{21}) > 0$ indicate the capacitive coupling, while the curves in the region of $\text{img}(Y_{21}) < 0$ represent the inductive coupling. When $\text{img}(Y_{21}) = 0$, there is a transmission zero. In this context, a passband appearing at the region of 4.5-5.5 GHz is denoted by the dotted line in Fig.6. In detail, when a slot $a = 36$ mm is chosen, a TZ is created in the lower stopband at around 4.0 GHz. On the contrary, when a coupling slot of $a = 21$ mm is chosen, a TZ appears in the upper-stopband at around 7.6 GHz.

III. MULTI-MODE CAVITY FILTERS WITH UPPER STOPBAND TZs

In this section, the proposed multi-mode resonator with slot structure introduced in Section II is utilized to present the first wideband multi-mode filter, namely, Type-I, with improved out-of-band performance by producing the TZs in the upper-stopband. The input/output ports of the filter are fed by the

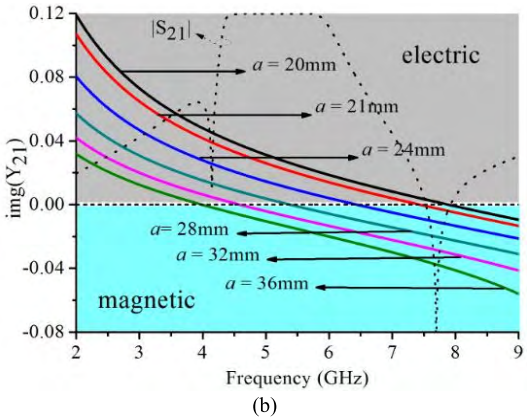

FIGURE 6. Imaginary part of the mutual admittance Y_{21} of the proposed slot structure with varying a when $h = 7.2$ mm and $b = 0.6$ mm.

coaxial cable probe. The h of the dual-, triple- and quadruple-mode filters are all set as 7.2 mm for the purpose of low profile.

$$Z_0 = \frac{30}{\sqrt{\epsilon_r}} \ln\left\{1+\frac{4}{\pi}\frac{b-t}{W'} \times \left[\frac{8}{\pi}\frac{b-t}{W'}+\sqrt{\left(\frac{8}{\pi}\frac{b-t}{W'}\right)^2+6.27}\right]\right\} \quad (1)$$

$$\frac{W'}{b-t} = \frac{W}{b-t} + \frac{\Delta W}{b-t} \quad (2)$$

$$\frac{\Delta W}{b-t} = \frac{x}{\pi\,(1-x)}\left\{1-\frac{1}{2}\ln\left[\left(\frac{x}{2-x}\right)^2+\left(\frac{0.0796x}{\frac{W}{b}+1.1x}\right)^m\right]\right\} \quad (3)$$

$$m = 2\left[1+\frac{2}{3}\frac{x}{1-x}\right] \quad (4)$$

$$x = \frac{t}{b} \quad (5)$$

A. DUAL-MODE FILTER

According to the results in Fig. 6, we can figure out that one slot coupling structure can create one TZ, and its frequency is mainly controlled by the slot length (a). Herein, $a = 21$ mm is chosen to create a TZ at about 7.7 GHz in dual-mode filter, meanwhile the resonant frequency of mode 2 (TE_{101}) shifts close to mode 1 resulting from the loaded slot as shown in Fig. 3(b). To elaborate the dual-mode filter established in Fig. 7(a), a circuit model is proposed in Fig. 7(b). The characteristic impedance of transmission line sections between the slots can be extracted from the physical structure by formula (1)-(5) [17].

Herein, W is the effective width of the inserted metal plane. As can be observed in Fig.8, the current density of the fundamental mode concentrates at the center portion of the metal plane. The reason is that there are two virtual magnetic planes or open circuits occur near the center portion of the metal plane as shown in the dotted line of Fig.8.

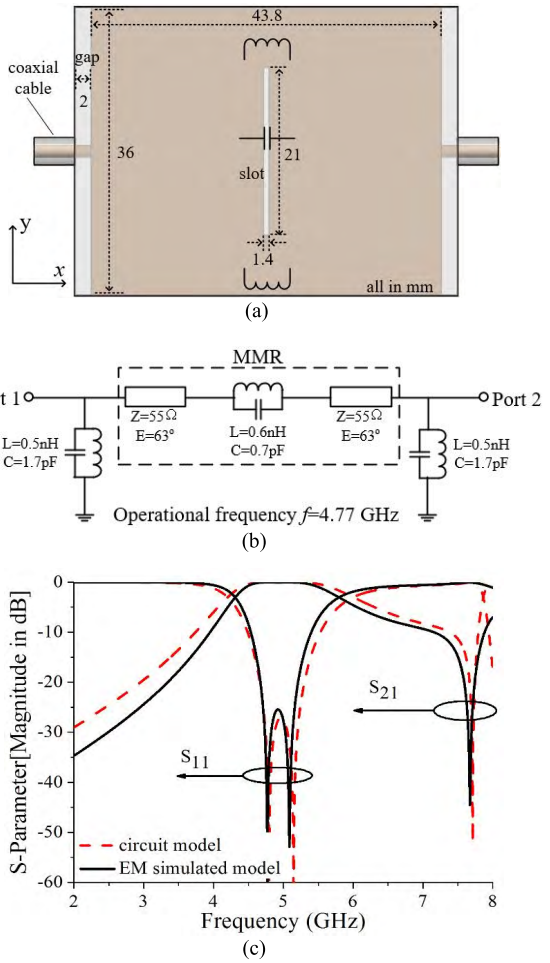

FIGURE 7. Dual-mode bandpass filter: (a) EM simulated model; (b) circuit model; (c) frequency responses.

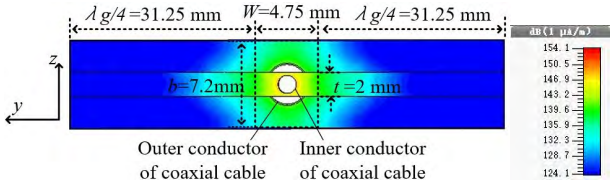

FIGURE 8. Electrical field distribution at cross-view ($x = 0$mm) of dual-mode filter.

These two dotted lines are in quarter-wavelength from the short-circuited side of the metal plane with respected to the fundamental mode frequency at $\lambda/4 = 31.25$ mm. Thus, the effective width of the metal plane can be calculated as $W = 4.75$ mm in this structure. Meanwhile b and t are equal to 7.2 mm and 2 mm, respectively. By substituting these parameters into (1)-(5), the characteristic impedance can be calculated as $Z = 55\ \Omega$. From Fig. 7(c), the frequency response of circuit model coincides well with the response of physical layout. The frequency response shows that the circuit model can effectively depict the physical dual-mode filter. The transmission zero is generated by the slot

structure in physical layout, which is caused by the resonance in a parallel LC circuit in the circuit model. The two shunt LC circuits represent the two gaps at the input/output feeding.

B. TRIPLE-MODE FILTER

A triple-mode filter is designed by two slots embedded on the inserted metal plane. The eigen- or resonant-frequencies of mode 1 (TE_{100}), mode 2 (TE_{101}) and mode 3 (TE_{102}) can be mainly controlled by the slot length (a) and distance (s) of two slots as shown in Fig.4. Herein, a slot length is set as 21 mm to achieve the two transmission zeros locating on upper-stopband, specifically, the first TZ is at about 7.9 GHz. Similarly to the dual-mode filter, a circuit model of triple-mode filter can be derived as presented in Fig. 8(b). There is one shunt capacitor at the center of the circuit to model the coupling between two slots for separating these two transmission zeros of the two identical adjacent slots. The calculated S-parameter of circuit model is plotted in Fig. 8(c), and the frequency response is in good agreement with that from the physical layout, which is utilized to further elaborate the transmission zeros generated by the slot structure and the triple-mode resonator.

In our triple-mode filter design, the external quality factor Q_e and coupling coefficient k are extracted as shown in Fig. 10. One can use these design curves to establish the coupling matrix for filter design. It is noteworthy that the external quality factor is small enough to construct the wideband triple-mode filter. Finally, the triple-mode filter is designed with the fractional bandwidth of 30% and the central frequency of 5 GHz with two transmission zeros on the upper-stopband.

C. QUADRUPLE-MODE FILTER

Fig. 11(a) indicates the layouts and dimensions of the quadruple-mode filter with two TZs on the upper-stopband, namely, Type-I. The circuit model is established in Fig. 11(b), the frequency response of quadruple-mode filter is presented in Fig. 11(c). The circuit model can be utilized to explain the multi-mode structure, which further confirms the discussion in design of dual- and triple-mode filters. The relevant external quality factor and coupling coefficient of quadruple-mode Type-I filter are extracted as plotted in Fig. 12. Finally, the quadruple-mode filter is designed at center frequency of 5 GHz with the bandwidth of 30%. There are two transmission zeros located at the upper-stopband. One is from the two identical non-adjacent slots and the other comes from the slot with larger width at the center of the circuit. It is noteworthy that the coupling between two identical slots are negligible due to the non-adjacent physical property. Thus, no shunt capacitor should be added in this circuit model.

Based on the above discussion, it can be seen from the return-loss in Fig. 7(c), Fig. 9(c), and Fig. 11(c) that the first mode (TE_{100}) of the dual-, triple- and quadruple-mode filters all fall in 4.8 GHz. The higher modes are evenly located within the passband. In this way, a class of multi-mode filters is established with transmission zeros at upper-stopband.

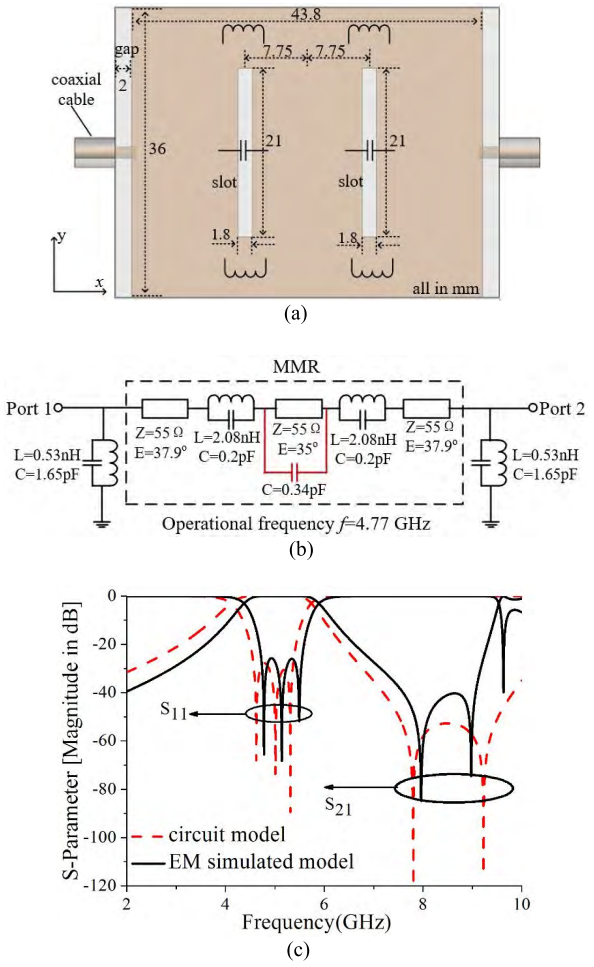

FIGURE 9. Triple-mode bandpass filter: (a) EM simulated model; (b) circuit model; (c) frequency responses.

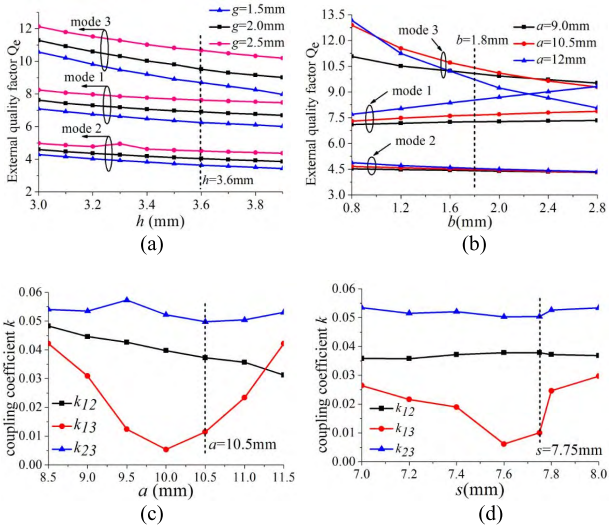

FIGURE 10. Triple-mode filter. (a) External quality factor Q_e with varied h and g. (b) External quality factor Q_e with varied a and b. (c) Coupling coefficient k with varied a. (d) Coupling coefficient k with varied s.

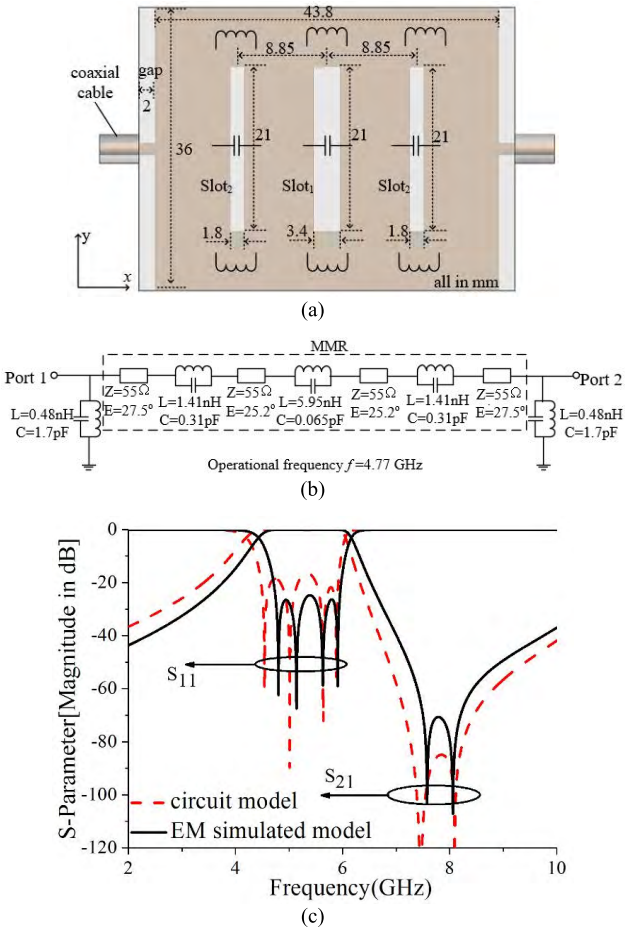

FIGURE 11. Quadruple-mode Type-I filter: (a) EM simulated model. (b) Circuit model; (c) frequency response.

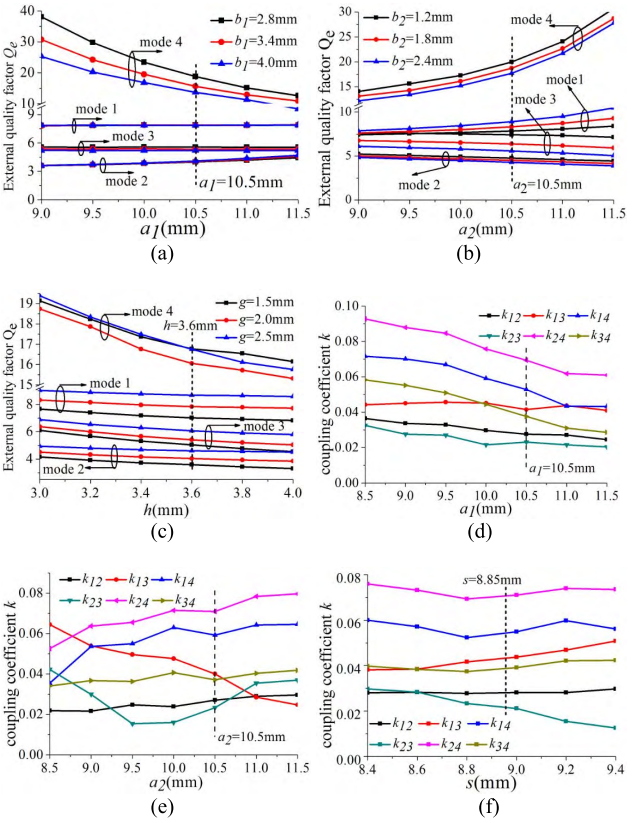

FIGURE 12. Quadruple-mode Type-I filter. (a) External quality factor Q_e with varied a_1 and b_1. (b) External quality factor Q_e with varied a_2 and b_2. (c) External quality factor Q_e with varied h and g. (d) Coupling coefficient k with varied a_1. (e) Coupling coefficient k with varied a_2. (f) The coupling coefficient k with varied s.

IV. MULTI-MODE CAVITY FILTER WITH IMPROVED OUT-OF-BAND

In this section, the second quadruple-mode filter is presented to further enhance its out-of-band suppression and achieve its size miniaturization, namely, Type-II, with both lower and higher transmission zeros. It is noteworthy that we use the single slot mixed coupling to realize lower-stopband TZs instead of traditional cross coupling method. To achieve the size reduction, a length of cavity (m) is chosen to be smaller. As shown in Fig. 2(f), a smaller value of m would lead to all the resonant modes separate apart. As also discussed in Section II, the introduction of slot-cuts would move the first four resonant modes close to each other and remain the fifth resonant mode apart from the passband. Fig. 13(a) depicts the layout of the designed quadruple-mode Type-II filter, of which the circuit model is given in Fig. 13(b). The frequency response from the circuit model is in good agreement with that from its physical layout, which is presented in Fig. 13(c). The photograph of the fabricated filter is given in Fig. 13(d). The filter is made of brass. The simulated and measured results are depicted in Fig. 13(e). The measured group delay is flat within the passband showing a good linearity. The measured passband has its central frequency of 5 GHz and fractional bandwidth of 30%. Meanwhile, the measured insertion loss in the passband is better than 0.6 dB and the attenuation in the out-of-band is lower than 15 dB. In this filter, one transmission zero appears at 4 GHz on the lower transition, and it is generated by the $slot_1$ at the center of the metal plane as shown in Fig. 13(a). As discussed in Fig. 6, the longer the slot is, the lower the transmission zero will be. Using this approach, the length of the $Slot_1$ is chosen as 36 mm for the transmission zero to be located at 4 GHz. By choosing the length of $Slot_2$ as 21 mm, the transmission zero is located at around 7.8 GHz as shown in Fig. 6. These transmission zeros are working together to improve the out-of-band suppression and selectivity of this filter when comparing with the Type-I filter with the same number of filtering order. Moreover, the length of the Type-II filter is 19% shorter than the Type-I filter.

V. DUPLEXER ON TWO INDIVIDUAL CAVITY FILTERS

In this section, the two individual quadruple-mode filters with wide upper-stopband and good frequency selectivity, developed in Section IV, will be utilized to construct a duplexer with its geometry shown in Fig. 14(a). The common feeding port, namely, Port-1, is formed through

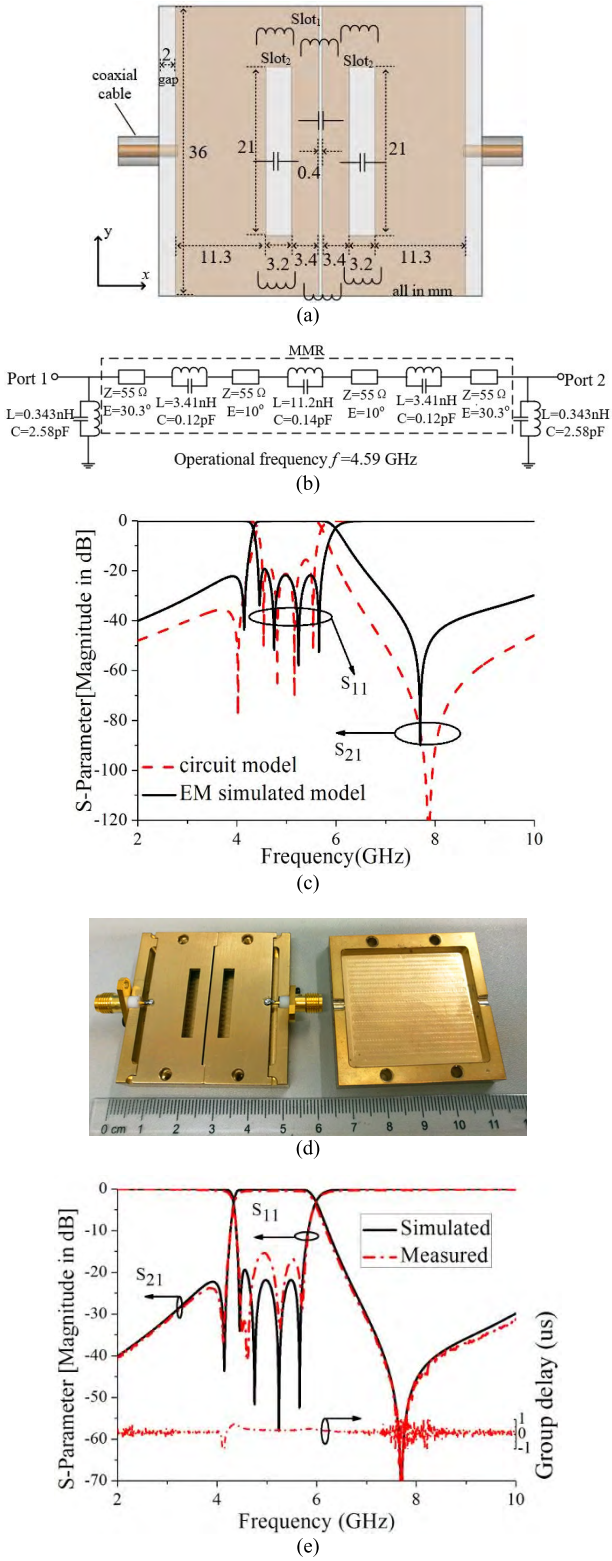

FIGURE 13. Quadruple-mode Type-II filter: (a) EM simulated Layout; (b) Circuit model; (c) Frequency responses of circuit model and physical layout; (d) Photograph of the fabricated circuit; (e) Measured and simulated frequency responses.

a T-junction structure by coaxial cable, and it is used to feed two filters with two different frequency passbands or channels, i.e., 2.9-3.9 GHz and 4.2-5.2 GHz. The work in [18]

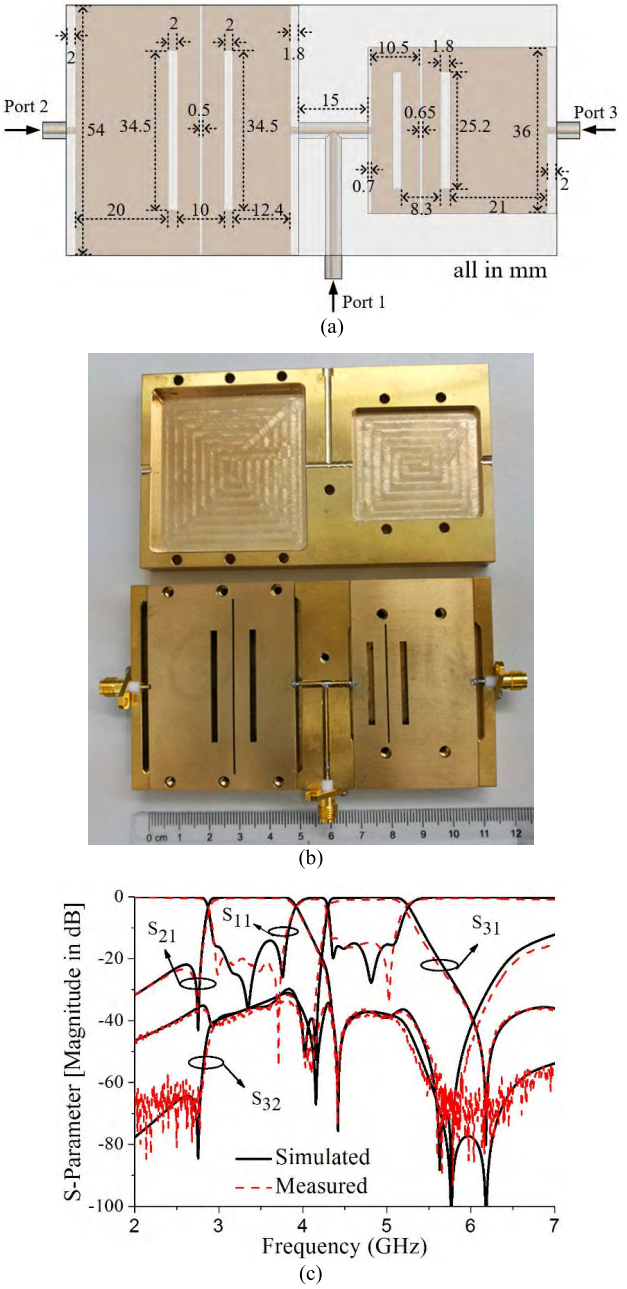

FIGURE 14. (a) Layout of duplexer. (b) Photograph of the fabricated duplexer. (c) Frequency responses of duplexer.

elaborates an iterative approach for optimal design of this duplexer with good impedance matching property. This approach is carried out on designing of each individual filter by obtaining the impedance in each filtering channel. According to the study in [18], it can be understood that the length of adjacent metal plane can be adjusted and employed to achieve the good impedance matching for the whole duplexer. After our optimal design is executed, this duplexer is fabricated with its photograph displayed in Fig.14 (b), and its simulated and measured results are plotted in Fig. 14(c).

First of all, it is found that this duplexer has achieved an excellent isolation between the two channels as illustrated in

both the simulated and measured results in Fig. 14(c). In our design, the two distinctive filtering channels are connected in shunt by using a T-shaped feeding circuit, and the whole structure is integrated and implemented on the brass only. The lower frequency channel of the developed duplexer has a center frequency at 3.4 GHz with its fractional bandwidth of 29.4%, while the higher frequency channel has a center frequency at 4.7 GHz with fractional bandwidth of 21.3%. Each filtering channel has its own TZs in both the lower- and upper-stopbands so as to realize its high filtering selectivity. In particular, a TZ appears at 4.4 GHz in the lower frequency channel, and a TZ emerges at 4.0 GHz in the higher frequency channel. These two individual TZs allow this proposed duplexer to achieve good isolation between two filtering channels as highly expected. In addition, the measured insertion losses in the lower and higher frequency passbands or channels achieve less than 0.9 dB. They are found in good agreement with their simulated results as well revealed in Fig. 14(c).

VI. CONCLUSION

In this paper, a concept using the higher harmonic modes and the metal plane inserted cavity to construct the multi-mode resonator is proposed. The quasi-elliptic multi-mode bandpass cavity filters and duplexer with slot loaded structure have been presented and designed to validate the concept. The proposed cavity filters have been exhibited to have low-profile geometry, low insertion loss, compact size and wideband filtering performance with sharpened out-of-band skirt. Meanwhile, a wide upper-stopband of 6.5-10 GHz has been well achieved with about 20 dB rejection. Based on the proposed filter structure, a wideband duplexer is accordingly developed with excellent filtering selectivity and high channel-to-channel isolation exceeding 30 dB. In the end, two quadruple-mode filters and their constituted duplexer have been designed and fabricated. Good agreement between the simulated and measured results has evidently validated the predicted performance.

REFERENCES

[1] L. Zhu, S. Sun, and W. Menzel, "Ultra-wideband (UWB) bandpass filters using multiple-mode resonator," *IEEE Microw. Wireless Compon. Lett.*, vol. 15, no. 11, pp. 796–798, Nov. 2005.

[2] S. W. Wong and L. Zhu, "Quadruple-mode UWB bandpass filter with improved out-of-band rejection," *IEEE Microw. Wireless Compon. Lett.*, vol. 19, no. 3, pp. 152–154, Mar. 2009.

[3] Q.-X. Chu and H. Wang, "A compact open-loop filter with mixed electric and magnetic coupling," *IEEE Trans. Microw. Theory Techn.*, vol. 56, no. 2, pp. 431–439, Feb. 2008.

[4] S.-B. Zhang, L. Zhu, and R. Weerasekera, "Synthesis of inline mixed coupled quasi-elliptic bandpass filters based on λ/4 resonators," *IEEE Trans. Microw. Theory Techn.*, vol. 63, no. 10, pp. 3487–3493, Oct. 2015.

[5] W.-C. Tang and S. K. Chaudhuri, "A true elliptic-function filter using triple-mode degenerate cavities," *IEEE Trans. Microw. Theory Techn.*, vol. MTT-32, no. 11, pp. 1449–1454, Nov. 1984.

[6] S. J. Fiedziuszko, "Dual-mode dielectric resonator loaded cavity filters," *IEEE Trans. Microw. Theory Techn.*, vol. MTT-30, no. 9, pp. 1311–1316, Sep. 1982.

[7] X.-X. Liang, K. A. Zaki, and A. E. Atia, "Dual mode coupling by square corner cut in resonators and filters," *IEEE Trans. Microw. Theory Techn.*, vol. 40, no. 12, pp. 2294–2302, Dec. 1992.

[8] H. Salehi, T. Bernhardt, T. Lukkarila, and S. Amir, "Analysis, design and applications of the triple-mode conductor-loaded cavity filter," *IET Microw. Antennas Propag.*, vol. 5, no. 10, pp. 1136–1142, Jul. 2010.

[9] V. Walker and I. C. Hunter, "Design of triple mode $TE_{01}\delta$ resonator transmission filters," *IEEE Microw. Wireless Compon. Lett.*, vol. 12, no. 6, pp. 215–217, Jun. 2002.

[10] R. R. Bonetti and A. E. Williams, "Application of dual TM modesto triple- and quadruple-mode filters," *IEEE Trans. Microw. Theory Techn.*, vol. MTT-35, no. 12, pp. 1143–1149, Dec. 1987.

[11] S.-W. Wong, Z.-C. Zhang, S.-F. Feng, F.-C. Chen, L. Zhu, and Q.-X. Chu, "Triple-mode dielectric resonator diplexer for base-station applications," *IEEE Trans. Microw. Theory Techn.*, vol. 63, no. 12, pp. 3947–3953, Dec. 2015.

[12] S.-W. Wong, S.-F. Feng, L. Zhu, and Q.-X. Chu, "Triple- and quadruple-mode wideband bandpass filter using simple perturbation in single metal cavity," *IEEE Trans. Microw. Theory Techn.*, vol. 63, no. 10, pp. 3416–3424, Oct. 2015.

[13] X. Wang, G. Jang, B. Lee, and N. Park, "Compact quad-mode bandpass filter using modified coaxial cavity resonator with improved *Q*-factor," *IEEE Trans. Microw. Theory Techn.*, vol. 63, no. 3, pp. 965–975, Mar. 2015.

[14] D. R. Hendry and A. M. Abbosh, "Analysis of compact triple-mode ceramic cavity filters using parallel-coupled resonators approach," *IEEE Trans. Microw. Theory Techn.*, vol. 64, no. 6, pp. 2529–2537, Aug. 2016.

[15] K. Gong, W. Hong, Y. Zhang, P. Chen, and C. J. You, "Substrate integrated waveguide quasi-elliptic filters with controllable electric and magnetic mixed coupling," *IEEE Trans. Microw. Theory Techn.*, vol. 60, no. 10, pp. 3071–3078, Oct. 2012.

[16] H. Wang and Q. X. Chu, "An inline coaxial quasi-elliptic filter with controllable mixed electric and magnetic coupling," *IEEE Trans. Microw. Theory Techn.*, vol. 57, no. 3, pp. 667–673, Mar. 2009.

[17] H. A. Wheeler, "Transmission-line properties of a strip line between parallel planes," *IEEE Trans. Microw. Theory Techn.*, vol. MTT-26, no. 11, pp. 866–876, Nov. 1978.

[18] J. S. Hong and M. J. Lancaster, *Microstrip Filters for RF/Microwave Applications*. New York, NY, USA: Wiley, 2001.

[19] P. Zhao and K. L. Wu, "An iterative and analytical approach to optimal synthesis of a multiplexer with a star-junction," *IEEE Trans. Microw. Theory Techn.*, vol. 62, no. 12, pp. 3362–3369, Dec. 2014.

BING-LONG ZHENG was born in Quanzhou, China. He received the B.E. degree in electronic information engineering from the Dalian Maritime University in 2015. He is currently pursuing the M.E. degree with the South China University of Technology, Guangzhou, China. His research interests include RF and microwave components.

SAI-WAI WONG (S'06–M'09–SM'14) received the B.S. degree in electronic engineering from The Hong Kong University of Science and Technology, Hong Kong, in 2003, and the M.Sc. and Ph.D. degrees in communication engineering from Nanyang Technological University, Singapore, in 2006 and 2009, respectively.

From 2003 to 2005, he was the Lead at the Engineering Department in mainland of China with two manufacturing companies in Hong Kong. From 2009 to 2010, he was a Research Fellow with the Institute for Infocomm Research, Singapore. In 2016, he was a Visiting Professor with The City University of Hong Kong, Hong Kong. From 2010 to 2016, he was an Associate Professor and became a Full Professor with the School of Electronic and Information Engineering, South China University of Technology, Guangzhou, China, in 2016. Since 2017, he has been a Full Professor with the College of Information, Shenzhen University, Shenzhen, China. His current research interests include RF/microwave circuit and antenna design.

Dr. Wong was a recipient of the New Century Excellent Talents in University Award in 2013. He is a Reviewer for several top-tier journals.

SHI-FEN FENG (S'15) was born in Jiujiang, China, in 991. He received the B.S. degree in information engineering from South China Agricultural University, Guangdong, China, in 2014, the M.E. degree in electronic and information engineering from the South China University of Technology, Guangzhou, China. He is currently an Engineer at Huawei Technologies Co., Ltd. His research interests include cavity microwave filters and diplexers design.

LEI ZHU (S'91–M'93–SM'00–F'12) received the B.Eng. and M.Eng. degrees in radio engineering from the Southeast University, Nanjing, China, in 1985 and 1988, respectively, and the Ph.D. degree in electronic engineering from the University of Electro-Communications, Tokyo, Japan, in 1993.

From 1993 to 1996, he was a Research Engineer with the Matsushita-Kotobuki Electronics Industries Ltd., Tokyo, Japan. From 1996 to 2000, he was a Research Fellow with the Faculty of Engineering, Ecole Polytechnique de Montreal, University of Montreal, Montreal, QC, Canada. From 2000 to 2013, he was an Associate Professor with the School of Electrical and Electronic Engineering, Nanyang Technological University, Singapore. Since 2013, he has been a Professor with the Faculty of Science and Technology, University of Macau, Macau, China, where he has been serving as the Head of the Electrical and Computer Engineering Department since 2014.

He has authored or co-authored 246 papers in peer-reviewed journals and conference proceedings, including 80 papers in the IEEE transactions/letters/magazine. His published papers have been cited over 3088 times with the H-index of 31 and average citations per paper of 18.18 (source: ISI Web of Science). His research interests include microwave circuits, antenna technique, and applied electromagnetics.

Prof. Zhu has been a member of the IEEE MTT-S Technical Committee on Computer-Aided Design since 2006 and the IEEE MTT-S Fellow Evaluation Committee since 2013. He was a recipient of the 1997 Asia-Pacific Microwave Prize Award, the 1996 Silver Award of Excellent Invention from the Matsushita-Kotobuki Electronics Industries Ltd., and the 1993 First-Order Achievement Award in Science and Technology from the National Education Committee, China. In, 2011, he was elevated to the IEEE Fellow for contributions to modeling, design and development of planar microwave filters. He served as the General Chair of the 2008 IEEE MTT-S International Microwave Workshop Series on the Art of Miniaturizing RF and Microwave Passive Components, Chengdu, China, and the Technical Program Committee Co-Chair of the 2009 Asia-Pacific Microwave Conference, Singapore. He was an Associate Editor for the IEEE TRANSACTIONS ON MICROWAVE THEORY AND TECHNIQUES from 2010 to 2013, an Associate Editor for the IEEE MICROWAVE AND WIRELESS COMPONENTS LETTERS from 2006 to 2012, and an Associate Editor for the *IEICE on Electronics* from 2003 to 2005.

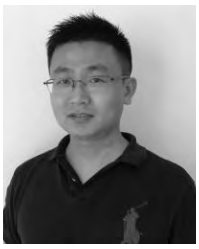

YANG YANG (S'11–M'14) received the Ph.D. degree from Monash University, Clayton VIC, Australia, in 2013. From 2012 to 2015, he was an Asia-Pacific GSP Engineer at Rain Bird. He was a Global GSP Success Award holder in 2014. He served as a Senior Research Associate with the Department of Engineering, Macquarie University from 2015 to 2016. In 2016, he was a Research Fellow with the State Key Laboratory of Millimeter-Waves, City University of Hong Kong. Since 2016, he has been the Lecturer with the University of Technology Sydney. His research interests include microwave and millimeter-wave circuits, reconfigurable antennas, wearable antennas, biosensors, and sensing technology.